Chapter 18

Directed Modification of Reaction Centers from Purple Bacteria

JoAnn C. Williams and James P. Allen*
Department of Chemistry and Biochemistry and Center for Bioenergy & Photosynthesis, Arizona State University, Tempe AZ 85287-1604, U.S.A.

Summary

Reaction centers from purple bacteria form a superb test system for the manipulation of electron transfer parameters. The wealth of cofactors and electron transfer reactions provides opportunities for directed modification of specific properties. In particular, the energies of each cofactor can be selectively changed by mutations of neighboring amino acid residues. The starting point for the initial electron transfer, the bacteriochlorophyll dimer, has proven to be exceptionally malleable, allowing large changes in energetics and rates. Most of the other cofactors can be exchanged or eliminated entirely, permitting considerable alteration of pathways. By orchestrating multiple changes in the reaction center, the light-initiated electron transfer pathway can be directed towards alternate ends, for example down the B branch of cofactors rather than the naturally preferred A branch. Extensive modeling of features of electron transfer such as the energetics, the coupling, and the protein dynamics has been corroborated by observed changes in the characteristics of the reactions after modification of the cofactor properties. For example, the maximum rates for several electron transfer reactions, determined by application of Marcus theory to the rates of reactions in a range of mutants, show a correlation with the

*Author for correspondence, email: JAllen@asu.edu

C. Neil Hunter, Fevzi Daldal, Marion C. Thurnauer and J. Thomas Beatty (eds): The Purple Phototrophic Bacteria, pp. 337–353.

distance between the cofactors. Other measurements revealing the intimate interaction of the protein and cofactors show that protein motion controls the rate of the initial electron transfer. Thus the reaction center provides a natural and modifiable template for understanding the factors governing electron transfer.

I. Introduction

What happens when the reaction center is excited by light? The light energy is converted into chemical energy through a series of electron and proton transfer reactions involving the cofactors of the reaction center. These reactions are able to proceed with essentially every light photon producing useful reactions, corresponding to a quantum efficiency of nearly 100%. The balancing act of capturing light energy while not destroying the molecules involved or producing unfavorable side reactions is achieved by fine tuning the properties of the cofactors through interactions with the protein in which they are embedded. The protein can influence several aspects of electron transfer identified by theoretical treatments, including the energetics, the coupling, and the protein dynamics. Although it is difficult to separate the contributions of each of these components, experiments have probed their effects, notably by altering the light-induced reactions in specific ways. This chapter will review the partnership between the cofactors and the protein scaffold as it relates to the parameters of electron transfer models, focusing on examples where changes in the properties have measurable effects on electron transfer. The examples will be primarily of reaction centers from *Rhodobacter* (*Rba.*) *sphaeroides* and *Rba. capsulatus*, the two commonly studied reaction center systems of purple bacteria.

II. Properties of the Cofactors

A. Identity, Substitution, and Removal

The reaction center from *Rba. sphaeroides* and *Rba. capsulatus* is an integral membrane protein complex composed of three proteins: the L, M, and H subunits. The L and M subunits form the core of the protein and are largely composed of five transmembrane helices that are structurally related to each other by an approximate two-fold symmetry axis. The H subunit is more peripheral, containing one transmembrane helix and a large cytoplasmic domain. Embedded in the middle of the L and M subunits are ten cofactors, all of which can participate in some manner in energy or electron transfer. The ten cofactors in the reaction center are: two bacteriochlorophyll *a* molecules that form a dimer (P), two bacteriochlorophyll *a* monomers (B_A and B_B), two bacteriopheophytin *a* molecules (H_A and H_B), two ubiquinone molecules (Q_A and Q_B), a carotenoid molecule, and an iron (Fig. 1). These cofactors are arranged into two branches, identified as the A and B branches, which are related by the same two-fold symmetry as found for the L and M subunits.

Although the cofactors are normally expressed with a well-defined composition, some of these cofactors can be substituted by molecules in the same class, for example bacteriochlorophylls for bacteriopheophytins. The monomer bacteriochlorophylls and bacteriopheophytins, the quinones, the carotenoid, and the iron can be biochemically removed and replaced. Mutagenesis can also result in biosynthetic substitutions, primarily by replacement of the amino acid residues coordinating the cofactors. For example, when the ligand to one of the central Mg atoms of P is changed, a bacteriopheophytin is incorporated rather than bacteriochlorophyll in a mutant that has been termed a heterodimer (His L173 to Leu and His M202 to Leu in *Rba. sphaeroides*, L173 and M200 in *Rba. capsulatus*) (Bylina and Youvan, 1988; Kirmaier et al., 1988; McDowell et al., 1991; Allen et al., 1996; van Brederode et al., 1999; King et al., 2001). Both halves of the dimer can be individually replaced this way, although the double bacteriopheophytin dimer appears to be unstable. Similarly the binding site for the B-side bacteriochlorophyll monomer is found to contain a bacteriopheophytin when the residue forming its Mg ligand is changed (ϕ mutant, His M182 to Leu in *Rba. sphaeroides*), although analogous mutations on the A side do not appear to have the same substitution effect (Katilius et al., 1999, 2004). Conversely, the bacteriopheophytin on the A side can be converted to bacteriochlorophyll by introduction of a residue to act as a ligand (β mutant, Leu M214

Abbreviations: B_A – bacteriochlorophyll monomer on A branch of cofactors; B_B – bacteriochlorophyll monomer on B branch of cofactors; H_A – bacteriopheophytin on A branch of cofactors; H_B – bacteriopheophytin on B branch of cofactors; P – bacteriochlorophyll dimer; Q_A – quinone on A branch of cofactors; Q_B – quinone on B branch of cofactors; *Rba.* – *Rhodobacter*

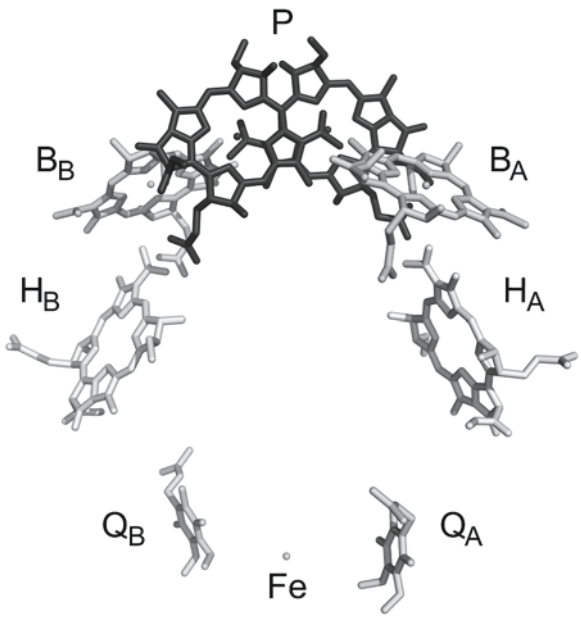

Fig. 1. Three-dimensional structure of the cofactors of the reaction center from *Rba. sphaeroides* R-26. Shown are the bacteriochlorophyll *a* dimer (P) (shaded dark), the two bacteriochlorophyll *a* monomers (B_A and B_B), the two bacteriopheophytin *a* molecules (H_A and H_B), the two ubiquinone molecules (Q_A and Q_B), and the iron (Fe). Although the carotenoid is present in wild type, it is not present in the R-26 strain. The view is perpendicular to the approximate two-fold symmetry axis that passes from P to Fe in the plane of the paper.

to His in *Rba. sphaeroides*, M212 in *Rba. capsulatus*) (Kirmaier et al., 1991). The addition of a histidine near the bacteriopheophytin on the B branch also results in incorporation of a bacteriochlorophyll (Leu L185 to His in *Rba. sphaeroides*) (Watson et al., 2005). Changing iron ligands results in a loss of metal specificity, and in one case a significant amount of zinc is incorporated (His M266 to Cys in *Rba. sphaeroides*) (Williams et al., 2007).

In addition to altering the cofactor composition, some of the cofactors can be removed or their incorporation can be blocked. Many studies of reaction centers have been performed on a carotenoid-less strain of *Rba. sphaeroides*, identified as R-26, which shows properties essentially identical to the carotenoid-containing wild type except for the loss of the ability to trap excess energy. The quinones can be taken out by exposing the reaction centers to a detergent treatment, which initially results in a decrease in Q_B followed by loss of Q_A. Biosynthetic incorporation of Q_A can be blocked by substitution of amino acid residues forming the binding pocket, for example by removing the tryptophan in van der Waals contact with Q_A (M252 in *Rba. sphaeroides* and M250 in *Rba. capsulatus*), or adding a tryptophan in place of a smaller residue (Ala M260 to Trp in *Rba. sphaeroides*) (Breton et al., 2004). Certain mutations near P result in reaction centers that lack a functional P (Val L157 to Arg, His L153 to Glu, Leu, Gln, or Tyr, His L173 to Gly, and His M202 to Gly in *Rba. sphaeroides*) (Jackson et al., 1997; Moore and Boxer, 1998; Katilius et al., 2004). The loss of H_A is one outcome of the large-scale alterations of the D_{LL} mutant, in which the D transmembrane sequence of the M subunit is replaced with the symmetry-related segment of the L subunit (M192 to M217 replaced with L165 to L190 in *Rba. capsulatus*) (Robles et al., 1990). Similarly, the B-branch bacteriopheophytin is not required for assembly of the reaction center as shown by a mutant with the change of an alanine that is adjacent to H_B to tryptophan (M149 in *Rba. sphaeroides*)(Watson et al., 2005). A loss of bacteriochlorophyll (presumably in the dimer) was also reported to be due to structural and electrostatic changes in a residue located between B_B and P (Ile L177 to His in *Rba. sphaeroides*) (Khatypov et al., 2005). See Chapter 16, Jones, for a summary of the effects of exclusion and replacement of reaction center cofactors. The ability to alter the cofactor composition provides the opportunity to manipulate the electron transfer reactions as discussed below.

B. Optical Spectra

One of the most accessible properties of the cofactors is the absorption spectrum (Fig. 2). The tetrapyrrole pigments (P, B_A, B_B, H_A, and H_B) have absorption peaks in the near-infrared region, the visible region and the UV region, and the quinones have an unresolved band in the visible region. The bacteriopheophytins, monomer bacteriochlorophylls, and dimer bacteriochlorophylls can be distinguished from each other in the near-infrared peaks at 760 nm, 800 nm, and 865 nm, respectively. In the visible region, the 540 nm peak arises from the bacteriopheophytins, and the 590 nm peak is from all four bacteriochlorophylls. The A and B branch pigments of the same type overlap, except at low temperature where the broad peak in the 540 nm region of the spectrum is resolved into two peaks at 533 nm and 546 nm associated with H_B and H_A, respectively. The contributions of the tetrapyrrole pigments in the Soret region have been delineated, with H contributing primarily on the

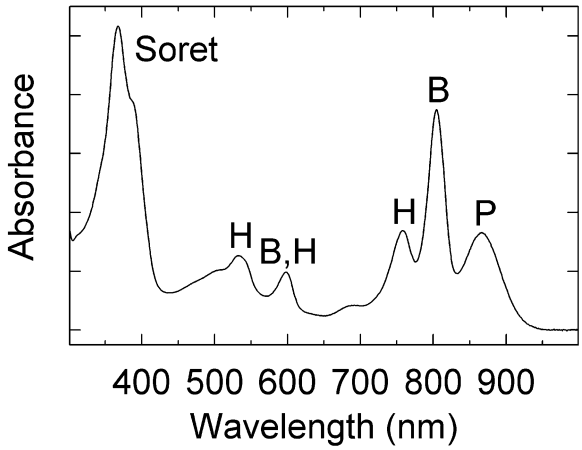

Fig. 2. Absorption spectrum of reaction centers from wild-type *Rba. sphaeroides*. The primary contributions of the bacteriochlorophyll dimer (P), bacteriochlorophyll monomers (B), and bacteriopheophytin monomers (H) to each of the absorption bands are identified. The Soret band arises from all the tetrapyrrole cofactors.

blue side and P absorbing on the red side (Wang et al., 2006). The carotenoid has a major but poorly resolved contribution to the absorption near 500 nm, where absorption of the other cofactors is weak, and can transfer excitation energy to the bacteriochlorophylls, performing a light-harvesting function in addition to photoprotection (Lin et al., 2003).

The absorption peaks in the near-infrared region are shifted from the solution spectra, notably in the shift of the bacteriochlorophyll bands to longer wavelengths, presumably because of their protein environment. However, specific alteration of the spectrum generally has not been amenable to mutagenesis. Modeling of the excited states has also proven difficult (Dahlbom and Reimers, 2005). However in certain instances, shifts in the spectrum are attributed to changing particular residues. A notable example is the change in the visible region peak of the bacteriopheophytins due to changing a hydrogen bond to the keto group of H_A, which established the assignment of these optical bands to the individual bacteriopheophytins (Bylina et al., 1988). However, changing a hydrogen bond is not typically correlated with a shift in the peak of the tetrapyrrole pigments. Another relatively malleable absorption peak is that of the dimer. It can shift up to approximately 15 nm to shorter wavelengths as a result of mutations, mostly mutations in which a hydrogen bond to the acetyl group is changed, precipitating a rotation of this side group. Major changes in the absorption spectra also occur when substitutions of the cofactors are introduced. For example, the near-infrared absorption peak of the dimer is significantly different in the heterodimer mutant. Likewise, shifts in the both the visible and near-infrared regions of the spectra are observed in mutants with alterations of ligands to the monomer bacteriochlorophylls that result in pigment changes (Katilius et al., 1999, 2004). Thus, the optical spectrum is a sensitive indicator of the effects of certain types of modifications to the reaction center.

The absorption bands in the near-infrared region arise from transitions from the ground state to the first excited state and so are markers of the excited state energy, indicating the maximum amount of energy that can be captured. For the primary donor of *Rba. sphaeroides*, the absorption peak at 865 nm corresponds to an energy difference of 1.4 eV. The properties of the reaction center can also be characterized from measurement of the spontaneous and stimulated emission of the excited state of the dimer, centered near 915 nm. Because the absorption and emission bands change as the cofactors undergo excitation, oxidation, and reduction, transient optical spectroscopy is one of the major techniques utilized to follow the light-induced transfer of electrons in the reaction center.

C. Oxidation/Reduction Midpoint Potentials

The oxidation/reduction midpoint potentials of the reaction center cofactors are critical properties for their function as electron transfer components. The midpoint potential of the dimer, at approximately 500 mV, is the only one easily measured directly (Fig. 3). The midpoint potentials of the other cofactors can only be inferred. A change in the chemical nature of a cofactor has a direct effect on its midpoint potential. For example, incorporation of a bacteriopheophytin in the heterodimer mutant increases the potential by approximately 130 mV due to the intrinsically higher potential of bacteriopheophytin (Allen et al., 1996). In addition, the energies of the electronic states are sensitive to the environment so protein interactions with the dimer, including hydrogen bonds and electrostatic forces from charged residues, can affect the dimer midpoint potential and be modulated by mutagenesis. The midpoint potentials of other tetrapyrroles in the reaction center can presumably also be changed by similar modifications, although the evidence is based upon alterations of the electron transfer rates rather than direct measurements.

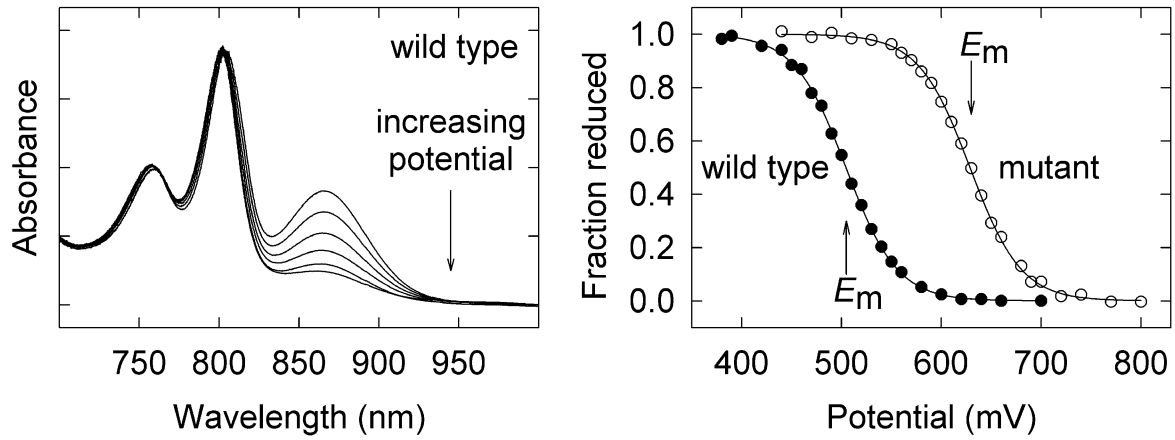

Fig. 3. (Left) The near-infrared region of the absorption spectrum showing a systematic decrease in the band associated with the bacteriochlorophyll dimer as the ambient potential is increased. The absorbance of this band is used to determine the fraction of P^+ at any given potential compared to the total amount of P. (Right) Fits of the dependence of the fraction of P^+ on the ambient potential are used to determine the oxidation-reduction midpoint potential, E_m. A shift in the midpoint potential is observed for a number of different mutants (Allen and Williams, 1995).

Whereas some modifications lead to large changes, analysis of various mutations indicates that most result in small (<50 mV) increases in the P/P^+ midpoint potential (Spiedel et al., 2002). The predominance of increases in the midpoint potential of P, rather than a mix of increases and decreases, is probably because the midpoint potential is poised by the protein interactions at a minimum value, and perturbations primarily disrupt this poise.

The effect of hydrogen bonds to the conjugated carbonyl molecules on the oxidation/reduction midpoint potential of the dimer is well documented (Allen and Williams, 1995, 2006). An additional hydrogen bond raises the potential by 60 to 120 mV while loss of the hydrogen bond present in the wild type decreases the potential by approximately 80 mV (Stocker et al., 1992; Williams et al., 1992; Murchison et al., 1993). Multiple systematic changes in the hydrogen bonding pattern produce a wide range of midpoint potentials (Lin et al., 1994a) and provide the opportunity to investigate the effect of altered energetics on the properties of the reaction center as discussed below. Hydrogen bonds have been introduced to the monomer bacteriochlorophylls, but with little effect on the primary photochemistry (Chen et al., 2004). A water molecule is found in the wild type between P and B_A in hydrogen bonding position to the keto carbonyl of B_A. This water molecule can be displaced by mutations (at M203 in *Rba. sphaeroides*), resulting in alteration in the electron transfer characteristics, including a slowing of the primary electron transfer rates, suggesting that B_A is more difficult to reduce, although other factors, such as an increase in the reorganization energy (see below), would also result in a slower rate (Potter et al., 2005; Yakovlev et al., 2005). Hydrogen bonds to bacteriopheophytins are also probably influencing their midpoint potentials. On the A side, a hydrogen bond between the 13^1 keto of H_A and a glutamic acid residue (L104 in *Rba. sphaeroides* and *Rba. capsulatus*) is naturally occurring, and the equivalent situation on the B side can be achieved by mutagenesis (Val M131 to Asp in *Rba. capsulatus*, M133 in *Rba. sphaeroides*) (Bylina et al., 1988; Müh et al., 1998; Kirmaier et al., 2002a). The presence of the hydrogen bonds most likely makes the bacteriopheophytins easier to reduce, consistent with the observed changes in electron transfer rates in the mutants.

The potential of each cofactor is also shaped by electrostatic interactions with charged and polar amino acid residues. Insertion or removal of ionizable residues at several different locations approximately 10 to 15 Å from P (L135, L155, L164, L170, L247 and M199 in *Rba. sphaeroides*) leads to a midpoint potential decrease up to 60 mV due to a negative charge and an increase up to 50 mV due to a positive charge (Williams et al., 2001; Johnson and Parson, 2002; Johnson et al., 2002). The effect of the charges on the potential is relatively modest because of screening of the charge-charge interactions by the surrounding protein. The energies of B_A and B_B can be significantly changed by altering the polarity of residues near

these tetrapyrroles, including replacing a conserved tyrosine residue with phenylalanine (M210 in *Rba. sphaeroides*, M208 in *Rba. capsulatus*), and changing a conserved phenylalanine to tyrosine (L181 in *Rba. sphaeroides* and *Rba. capsulatus*), as measured by changes in the electron transfer rates (Finkele et al., 1990; Nagarajan et al., 1990; Jia et al., 1993) and Stark spectra (Treynor et al., 2004). Theoretical calculations suggest that electrostatic fields near B_A and B_B are influenced by the polarity of these residues, and consequently mutations result in energetic shifts for the oxidized states (Alden et al., 1996; Gunner et al., 1996). In general, the sensitivity of the cofactors to specific protein interactions provides a means to test the role of the energies of the charge-separated states in determining the electronic structure of the cofactors and the rates of electron transfer as presented in the subsequent sections.

D. Modeling the Electronic Structure of the Bacteriochlorophyll Dimer

The close overlap of the two tetrapyrroles in P results in a sharing of the electron orbitals and hence changes in the properties of P compared to bacteriochlorophyll monomers. For example, one effect of the dimerization is a shift in the absorption band to a longer wavelength than is observed for the bacteriochlorophyll monomers. In a simple Hückel molecular orbital model, the two conjugated molecules can be considered to be coupled together, resulting in the electrons being distributed over the two bacteriochlorophylls in molecular orbitals that are split by an energy 2β (Fig. 4). An additional term represents the difference in the energies of the two sides arising from the inhomogeneous nature of the protein surrounding P. When P is oxidized, the higher molecular orbital loses an electron, leaving one unpaired electron. In the Hückel model, the predominant contribution to the higher molecular orbital is from the side with the higher energy (Plato et al., 1992). In the wild-type reaction center, measurement of the unpaired electron spin densities using the magnetic resonance technique called electron nuclear double resonance yields a 2:1 ratio for the spin density on the L side bacteriochlorophyll compared to the M side. The energy difference between the two sides can be manipulated by introduction of hydrogen bonds to P, resulting in systematic changes in the molecular energies and hence the ratio of the spin densities (Fig. 4) (Artz et al., 1997; Müh et al., 2002). In general, a hydrogen bond between the side chain of an amino acid residue and the M side of P stabilizes the energy of that side and increases the energy difference of the molecular orbitals, making the spin ratio more asymmetric. A hydrogen bond to the L side of P stabilizes that side and hence decreases the energy difference for the molecular orbitals and produces a more symmetrical spin distribution. In both cases, the additional hydrogen bond lowers the energy of the highest molecular orbital, which is coupled to the midpoint potential, making P more difficult to oxidize. More extensive modeling involving additional factors, such as the contribution of vibrational states, provides estimates for the positions of bands seen in the infrared region of the optical spectrum (Müh et

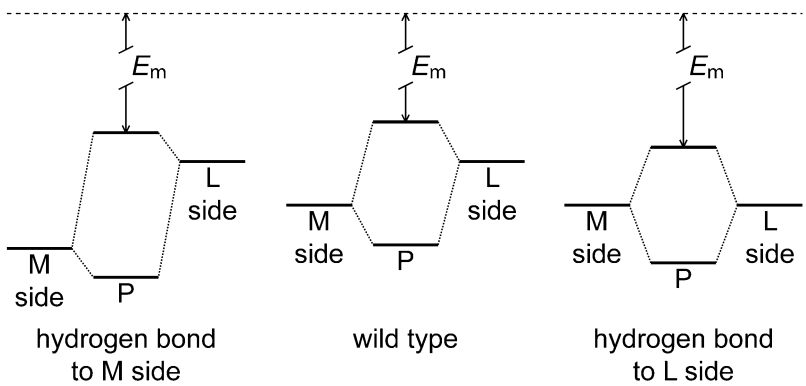

Fig. 4. A two-orbital Hückel model of the bacteriochlorophyll dimer. In wild type, the energy splitting of the molecular orbitals of P is determined by the energy difference between the two sides of P and the coupling. Mutations that introduce a hydrogen bond to the M side of P stabilize the energy of the M side bacteriochlorophyll, resulting in a more asymmetrical dimer with a larger energy difference for the molecular orbitals and a larger midpoint potential (E_m). Introducing a hydrogen bond to the L side results in a more symmetrical dimer while still increasing E_m.

al., 2002; Reimers and Hush, 2004; Kanchanawong et al., 2006).

In comparison to P in the bacterial reaction center, the electronic structure of the primary electron donor of Photosystem I, P700, is very asymmetrical with a ratio of at least 3:1 in spin density distribution over the two tetrapyrroles (Webber and Lubitz, 2001). Two factors contribute to this asymmetry. The primary donor has a heterodimeric nature as the B-side tetrapyrrole is a chlorophyll *a′*, which contains an epimeric configuration at the 13^2 position, rather than a chlorophyll *a* as found on the A side. Whereas both sides are axially coordinated by histidines, only the chlorophyll *a′* has a hydrogen bond (between Thr 739 of the PsaA subunit and the 13^1 position). The presence of this hydrogen bond likely stabilizes the chlorophyll *a′* side of P700 resulting in the chlorophyll *a* side having a much higher energy and hence a much larger unpaired spin density. Mutation of Thr 739 to Ala results in a 60 mV decrease in the oxidation/reduction potential while a 30 mV decrease is observed for a Val mutation (Witt et al., 2002; Li et al., 2004). Associated with the loss of the hydrogen bond is a small redistribution of the electron spin density from the B side to the A side of P700 as expected based upon the theoretical model. Thus, the understanding developed from the bacterial system appears to be applicable to other photosystems.

III. Electron Transfer Concepts

According to Marcus theory, the rate, *k*, of electron transfer between a donor and acceptor can be written in terms of the temperature, *T*, the effective electronic matrix element, or coupling, *V*, and energetics according to:

$$k = \sqrt{\frac{4\pi^3}{h^2 \lambda RT}}\, V^2\, e^{-\left(\frac{(\Delta G^\circ + \lambda)^2}{4\lambda RT}\right)} \qquad (1)$$

with two contributions to the energetics: the free energy difference between the final and initial states, ΔG°, and the reorganization energy, λ, which represents the rearrangement energy associated with the charge transfer (Marcus and Sutin, 1985). The exponential dependence of the rate on the energy terms is due to the activation energy associated with the process. Electrons can flow over long distances in biological systems because of a careful balance, mediated by the protein, involving the free energy difference, the reorganization energy and the coupling between distant redox cofactors. The factors that influence the energetics and coupling in protein complexes are considered below.

A. Energetics

The electron transfer rate has an exponential dependence upon the free energy difference and reorganization energy (Eq. 1). The free energy differences between various states formed during electron transfer steps in wild type range from relatively small values of approximately 200 meV for the initial electron transfer to a value of approximately 500 meV for charge recombination from the primary and secondary quinones. Mutants with altered P/P^+ midpoint potentials have corresponding changes in the free energy differences for the electron transfer steps. For example, a higher P/P^+ midpoint potential increases the free energy difference between the PQ_A ground state and the $P^+Q_A^-$ state. By measuring the rates for different mutants, the dependence of the electron transfer rates on the free energy difference can be experimentally determined. The dependence of the electron transfer rate typically is shown as the logarithm of the rate versus the free energy difference, yielding a parabolic curve (Fig. 5). The value of the free energy difference at the peak of the curve is equal to the reorganization energy, because for that value the exponential term has a maximal value of one. The rate at the peak of the parabola is proportional to the coupling for the reaction.

In principle, the energies of the cofactors, including their charged states, can be established by theoretical calculations based upon the three-dimensional structure of the protein. However, for large pigment-protein complexes, these efforts remain a challenge due to the large number of interactions and the uncertainties in the atomic positions often found in structural models that are limited by the resolution of the X-ray diffraction data. Electrostatic potentials calculated for the reaction center from *Blastochloris viridis* show a strong asymmetry in the electrostatic potential for the two branches, with the A branch being substantially more positive than the B branch, significantly favoring electron transfer along the A branch (Gunner et al., 1996). The oxidation/reduction midpoint potential for P680 of Photosystem II is calculated to have a significantly higher potential than P in bacterial reaction centers, in agreement with

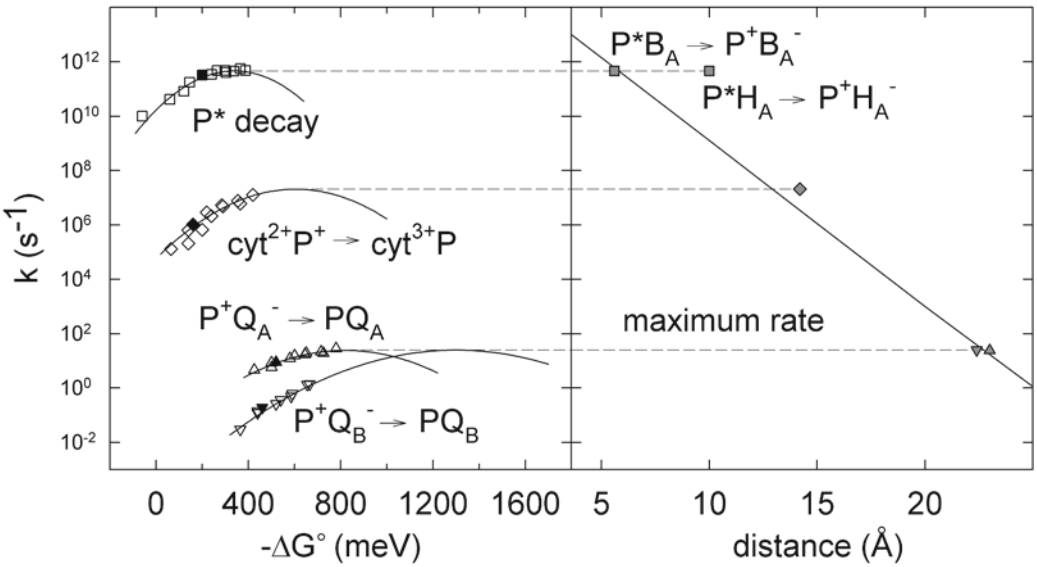

Fig. 5. (Left) The dependence of the electron transfer rate on the free energy difference for four reactions: the initial P* decay, electron transfer from bound cytochrome c_2 to P^+, and charge recombinations from the primary and secondary quinones. The lines are fits according to the Marcus relationship (Eq. 1). The data points and fits are from previous publications (Lin et al., 1994b; Allen et al., 1998; Haffa et al., 2002). (Right) The maximum rate from each fit is proportional to the coupling for the reaction and yields a rate that is predicted to be exponentially related to the separation distance between the electron donor and acceptor. For the P* decay, the maximum rate is plotted for transfer to two possible acceptors, B_A and H_A. The fit shown is from Dutton and coworkers (Noy et al., 2006).

the experimental data (Ishikita et al., 2006). These calculations also suggest that the specific orientation of the 13^2 ester of bacteriochlorophylls has a strong influence on the potential (Ishikita et al., 2005). Calculations making use of dynamics and alternate values for the dielectric constant result in different values for the potentials but are still in agreement with favorable transfer along the A branch (Parson et al., 1990; Gehlen et al., 1994).

Experimentally, the strength of the electrostatic fields can be established using a technique known as electroabsorption or Stark spectroscopy, in which changes in the optical spectrum due to the application of an electric field across a sample are measured. These optical changes can be interpreted in terms of the interactions of the applied electric field with the dipole moments of the cofactors. For the bacterial reaction center, such measurements lead to estimates of a strong field of 10^6 V/cm near the bacteriochlorophyll dimer (Middendorf et al., 1993). The electrostatic field around P changes by approximately 10% when comparing reaction centers with and without the carotenoid (Yanagi et al., 2005). Because the electron transfer rates are insensitive to the presence or absence of the carotenoid, the electrostatic field is not a major determinant for the directionality along the A branch.

Replacement of one of the coordinating histidine residues of P with leucine produces the heterodimer, while mutants with the histidine replaced with glycine are very similar to wild type in their properties, presumably due to the incorporation of water as a ligand in place of the histidine (M202 in *Rba. sphaeroides*) (Goldsmith et al., 1996). Likewise, replacement of the histidine coordinating B_A with a small amino acid residue (His L153 to Ser or Gly in *Rba. sphaeroides,* Thr or Ser in *Rba. capsulatus,* and Cys in *Blastochloris viridis*) results in mutants with properties that are very similar to those of wild type, while mutation to leucine alters the pigment composition (Bylina et al., 1990; Arlt et al., 1996; Katilius et al., 2004). Thus, these bacteriochlorophylls are tolerant of coordination changes, with the energetics of P and B_A being only weakly dependent upon the nature of the coordination.

Protein interactions such as hydrogen bonds to the intermediate electron acceptors also influence the energetics of electron transfer. Removal of the hydrogen bond between a glutamic acid residue (L104 in *Rba. sphaeroides* and *Rba. capsulatus*) and the keto group at the 13^1 position of H_A results in a small decrease in the forward electron transfer rate from P* (Bylina et al., 1988), consistent with a decrease in the free energy difference due to a change in the

energy of H_A^-. In Photosystem I, loss of the hydrogen bond between a tyrosine residue and either of the chlorophyll monomers located in positions analogous to H_A and H_B (Tyr 696 of the PsaA subunit near the 13^1 position of $ec3_A$ or Tyr 676 of the PsaB subunit near $ec3_B$) alters the electron transfer ratio of the two branches, suggesting that in Photosystem I, the rates are very sensitive to the energetics established by the pigment-protein interactions (Li et al., 2006).

B. Coupling

In addition to controlling the energies of the cofactors, the protein must provide an environment that establishes a suitable coupling, or formally the effective electronic matrix element, between the cofactors poised in their excited or charged states for the reactions. In theoretical models, coupling can be considered as arising from a pathway from the donor to the acceptor. In these models, the protein is considered to consist of a complex array of bonds as well as close but non-bonding contacts. A theoretical framework has been developed to express the protein as a network of covalent bonds, hydrogen bonds, and through-space jumps along which electron transfer proceeds in many steps (Lin et al., 2005; Gray and Winkler, 2005). Rather than making use of explicit calculations, coupling is more commonly estimated by assuming that the protein environment is relatively homogeneous, with the coupling being primarily dependent upon only the distance between the donor and acceptor (Gray and Winkler, 2005; Noy et al., 2006). In this simplified case, the coupling exponentially decreases with increasing separation (Fig. 5) showing that the maximal electron transfer rates can span a range of nearly 10^{12} s^{-1} for cofactors in close contact to a rate of 25 s^{-1} when the separation is 23 Å.

Because of the exponential dependence on distance, electron transfer in biological systems often makes use of a series of steps involving closely positioned cofactors rather than utilizing a single step between more distantly located cofactors. In order to meet the critical demands for efficient electron transfer, careful positioning of the cofactors and fine control of the energies of the cofactors is essential. For this reason, electron transfer in the reaction center from P* to Q_B involves a series of intermediate acceptors, B_A, H_A, and Q_A. In general, the initial steps have very fast electron transfer rates between closely aligned cofactors. The approximate two-fold symmetry for the two branches suggests comparable couplings as has been found by consideration of the relative rates in various mutants (Katilius et al., 2002b). Comparison of the P* to $P^+H_A^-$ and P* to $P^+H_B^-$ rates and free energy differences indicates that the slower rate for the B-branch transfer is not accounted for entirely by the energetics, and so the coupling does have a contribution, although modest (Kirmaier et al., 2001, 2005).

The charge recombination reactions illustrate how the maximal rate is primarily determined by the distance. In the wild type, the two quinones have observed recombination rates that differ by a factor of 10, although the two quinones are approximately equidistant from P. However, charge recombination from $P^+Q_B^-$ has a significantly larger reorganization energy than that from $P^+Q_A^-$, as evident by the peak of the parabola being at a higher free energy difference, resulting in very comparable maximum rates as predicted by their similar distances to P (Allen et al., 1998).

These theoretical models to describe electron transfer within proteins can be expanded to also understand electron transfer between cofactors found in two different proteins (Lin and Beratan, 2005; Lin et al., 2005; Miyashuta et al., 2005). In interprotein transfer, additional factors must be considered, such as the docking of the proteins and the involvement of water molecules at the protein interface. For example, cytochrome c_2 is a water-soluble protein that transfers an electron only after binding to the reaction center (Chapter 17, Axelrod et al.). In this case, coupling is established by the ability of interfacial water molecules to form multiple hydrogen bonding pathways that connect the tunneling pathways for each of the proteins (Miyashita et al., 2005).

C. Dynamics

The conventional Marcus theory (Eq. 1) rests on the assumption that the electronic transition from the initial to the final state is much faster than nuclear motion. Theories have been developed that explicitly account for dynamics (Sumi and Marcus, 1986; Warshel et al., 1989; Gehlen et al., 1994). However, dynamical contributions are rarely used because of difficulties in experimentally measuring the contributions. Although the initial electron transfer has been well characterized, including the free energy dependence for the rate (Haffa et al., 2002), certain aspects of the transfer have been puzzling. The kinetics of the changes in the spectra of the pigments are complex,

and the three-fold increase in the electron transfer rate as the temperature decreases from 298 to 4 K is unusual. To determine the contribution of dynamics to the initial rate, this reaction has been analyzed by probing nearby amino acid residues, measured by absorbance changes in tryptophan residues (Wang et al., 2007). These measurements show that the protein dynamics is the limiting factor in the initial electron transfer rate rather than the energetics. In the classical picture of electron transfer, the protein undergoes structural changes only after the electron transfer to the acceptor is complete (Fig. 6). This observed dependence on the dynamics shows that the protein motions occur during the process and control the observed rate by overcoming the activation barriers described in the classical Marcus theory.

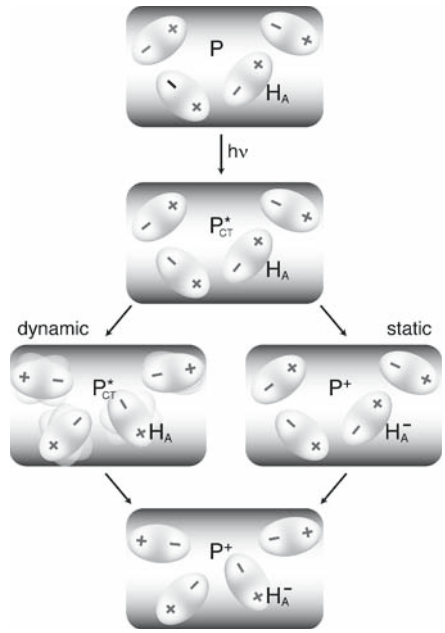

Fig. 6. Light results in formation of the charge-separated state $P^+H_A^-$ in reaction centers. In the traditional static view of electron transfer, the movement of dipoles from protein side chains and water molecules is considered to be very slow compared to the initial electron transfer rate. In contrast, in the dynamic model of the reaction center, dipoles rearrange in response to the light-induced formation of P^*_{CT}, the excited state of P, which has a charge-transfer character, followed by transfer of the electron. Recent measurements of the dynamics of the reaction center show that these rearrangements play a critical role in determining the rate of the electron transfer process (Wang et al., 2007).

IV. Pathways of Electron Transfer

A. B-side Electron Transfer

In wild-type reaction centers, electron transfer proceeds along the A branch with a nearly 100% efficiency. Manipulation of the various factors influencing electron transfer comes in most dramatically in experiments aimed at getting the electron to go the 'wrong' way. Mutations that increase B-branch electron transfer have been reviewed by Wakeham and Jones (2005). Achieving a significant amount of transfer along the B branch requires a combination of mutations, such as blocking the A side by mutations that prevent incorporation of Q_A or H_A, altering the energies of the A-side states to make electron transfer less favorable by mutations near B_A and H_A, and altering the energies of the B side states to make electron transfer more favorable by mutations near B_B (Fig. 7). Although reaction centers from *Rba. sphaeroides* and *Rba. capsulatus* have very similar electron transfer rates, the effect of many subtle differences involved in the branching is illustrated by a lower propensity of reaction centers from *Rba. sphaeroides* for electron transfer along the B branch (Kirmaier et al., 2002b). In early experiments on altering the branching ratios, only electron transfer to H_B was observed, but now transfer to Q_B has been achieved with reasonable efficiency.

The difference in the energy levels of the states $P^+B_A^-$ and $P^+B_B^-$ with respect to P* is an important factor in determining the branching ratio. Mutations that only increase the lifetime of P* are insufficient for switching to B-side electron transfer (de Boer et al., 2002). Changing the energetics along the two branches can be accomplished by the introduction of an aspartic acid residue near B_A (for Gly M201 in *Rba. capsulatus*, M203 in *Rba. sphaeroides*), showing that individual residues can influence the balance between A-side electron transfer, B-side electron transfer, and charge recombination (Heller et al., 1995). Similarly, a lysine residue introduced near B_B results in an alteration of the branching ratio (at Ser L178 in *Rba. capsulatus*) (Kirmaier et al., 1999), as does a combination of mutations that destabilizes P^+B_A and stabilizes P^+B_B (at L181 in *Rba. sphaeroides* and *Rba. capsulatus*, and at M210 in *Rba. sphaeroides*, M208 in *Rba. capsulatus*) (Kirmaier et al., 2004). The ϕ_B mutant, in which B_B is replaced with a bacteriopheophytin (because of the His M182 to Leu mutation in *Rba. sphaeroides*), is observed to form the state $P^+B_B^-$ with a yield of 35%, although no electron transfer to H_B is observed, probably because

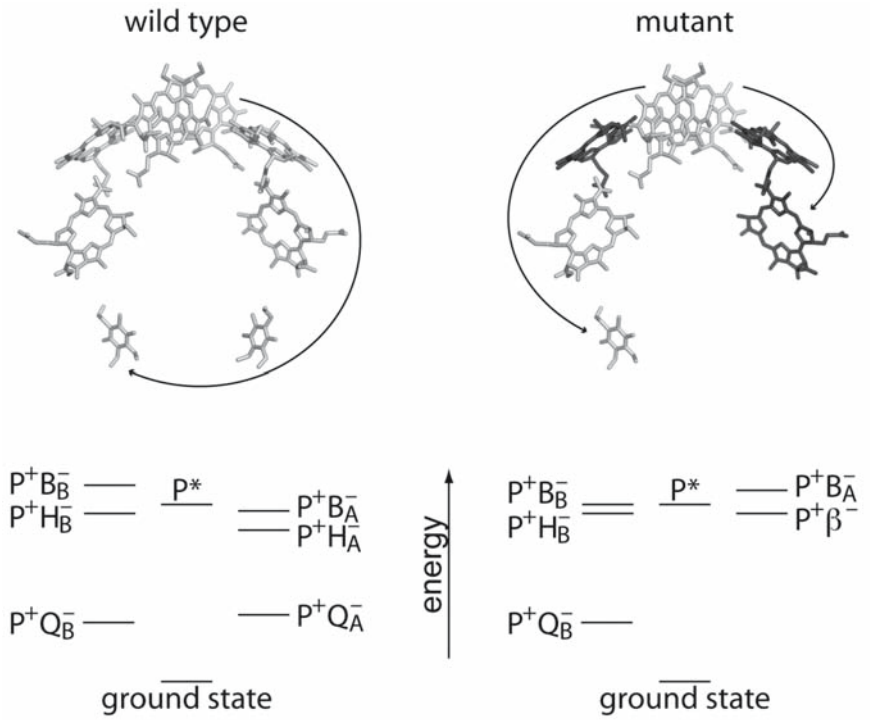

Fig. 7. In wild-type reaction centers, electron transfer occurs almost exclusively along the A branch of cofactors. In reaction centers with a set of four mutations, a significant percentage of electron transfer is observed to occur along the B side. For the YFHV mutant in *Rba. capsulatus* (Kirmaier et al., 2003), the Phe L181 to Tyr mutation lowers the energy of $P^+B_B^-$ while three changes make electron transfer along the A branch unfavorable: the Tyr M208 to Phe mutation raises the energy of B_A^-, the Leu M212 to His mutation results in H_A being replaced with a bacteriochlorophyll (β), and the Trp M250 to Val mutation prevents the incorporation of Q_A.

the state $P^+B_B^-$ is lower in energy than $P^+H_B^-$ (Katilius et al., 1999, 2002a,b, 2003). Thus raising the free energy of $P^+B_A^-$ and lowering the free energy of $P^+B_B^-$ has been key in promoting electron transfer down the B side to give $P^+H_B^-$.

Yields of $P^+H_B^-$ of greater than approximately 30% are accomplished by combining mutations near the monomer bacteriochlorophylls with mutants that impede electron transfer along the A branch. A number of these combination mutants incorporate the β mutation, in which H_A is replaced by a bacteriochlorophyll, resulting in a substantially higher energy for the $P^+\beta^-$ state compared to $P^+H_A^-$ (Kirmaier et al., 2002a, 2003; Kee et al., 2006). An exceptionally high yield of 70% $P^+H_B^-$ was achieved by joining together mutations that alter the energies of B_A and B_B with changes derived from the D_{LL} mutant, for which electron transfer along the A branch is blocked because of the lack of H_A in that mutant (Chuang et al., 2006). On the other hand, relatively small changes in the energies of H_A and H_B, such as by addition of a hydrogen bond to H_B to lower the energy level of $P^+H_B^-$, are insufficient to increase the yield of B-side transfer (Kirmaier et al., 2002a).

A number of mutants with changes near the bacteriochlorophylls and bacteriopheophytins produce $P^+H_B^-$ but do not have significant electron transfer to Q_B, attributed to the forward reaction being unable to compete with charge recombination (de Boer et al., 2002). The rate of electron transfer from $P^+H_B^-$ to $P^+Q_B^-$ is much slower than the rate from $P^+H_A^-$ to $P^+Q_A^-$, and so competes less well with charge recombination (Kirmaier et al., 2003; Kee et al., 2006). Several factors could influence the difference in the two rates (Kirmaier et al., 2003; Paddock et al., 2005). For example, the much larger reorganization energy associated with formation of Q_B^- compared to Q_A^-, as discussed above, would favor a much faster rate for Q_A^- formation. Also contributing could be the free energy differences for the bacteriopheophytin to quinone electron transfer on the two sides being slightly different. Although the bacteriopheophytin to quinone separation distances for the two sides are comparable, differences in the coupling are suggested

by distinct interactions of the quinones with nearby aromatic amino acid residues (Trp M252 in *Rba. sphaeroides* and M250 in *Rba. capsulatus* near Q_A and Phe L216 near Q_B).

Electron transfer can get all the way to Q_B via B-branch electron transfer if the A branch is blocked (Laible et al., 2003). Removal of Q_A also allows one to observe spectra of Q_B generated only by B-side transfer (de Boer et al., 2002; Breton et al., 2004; Paddock et al., 2005, 2006). The yield of Q_B^- when the A branch is blocked depends on what other mutations are present (Wakeham et al., 2003, 2004; Frolov et al., 2005). Mutations near Q_B that decrease the polarity (Glu L212 to Ala and Asp L213 to Ala in *Rba. sphaeroides*) increase the yield of Q_B^- by B-branch electron transfer, postulated to be either by changing the rate through altering the oxidation-reduction potential and therefore the driving force or altering the reorganization energy (Wakeham et al., 2003).

Although coupling has been modeled extensively, its effects on establishing the branching of electron transfer are somewhat difficult to measure experimentally, as it is not clear how to rationally change the spatial orbital overlaps. However, the heterodimer mutations afford a way to change the electron density distribution, which is also involved in the coupling. Mutants constructed by Kirmaier and coworkers (2005) to assess the coupling involve combining either the A or B side heterodimers and the β mutation that replaces H_A with a bacteriochlorophyll. This combination of mutations has the effect of making the states $P^+B_A^-$ and $P^+H_B^-$ approximately equal in energy (thus equalizing the free energy contribution) while raising the monomer states such that the mechanism (superexchange) of the initial electron transfer should be the same on both branches. Although the yield of B-side transfer is low in both cases, it is approximately four-fold less for the mutant with the A-side heterodimer. Because the energies for the heterodimer mutants with the bacteriochlorophyll on either side are assumed to be comparable, the difference in yields is attributed to a small but real difference in coupling of the dimer to H_A and H_B. This coupling difference should contribute to the A-side preference for electron transfer found in other mutants and wild type.

The pathway of electron transfer also appears to be dependent on the wavelength of the excitation energy. Blue light excitation into the Soret band gives rise to a transient $B_B^+H_B^-$ state, which decays in picoseconds at room temperature but is longer lived at low temperature (Lin et al., 2001; Haffa et al., 2003). Although energy transfer is fast, alternate photochemistry upon differing excitation wavelengths shows that energy transfer and electronic relaxation do not always precede electron transfer (Wang et al., 2006). These surrogate conduits for the dissipation of excitation energy suggest that the function of the B branch remains to rapidly quench higher excited states (Lin et al., 2001). Thus the B branch is poised to form charge-separated states but not to result in a terminal electron transfer as the A side is. This is consistent with the location of the carotenoid, also thought to be involved in photoprotection (Lin et al., 2003), on the B branch.

The pathway of electron transfer, in addition to being dependent on wavelength, can also be dependent upon electrostatic interactions involving a cofactor and a nearby charged amino acid residue. Introduction of protonatable residues (His L168 to Glu and Asn L170 to Asp in *Rba. sphaeroides*) results in a pH dependence for the states generated by light excitation (Haffa et al., 2004). Because the charges on the ionizable residues depend on their protonation state, and the protonation state is pH dependent, the pathway then becomes pH dependent, demonstrating an ability to switch the pathway by adjustment of the pH.

In summary, the highly efficient transfer of electrons along the A branch in wild type can be manipulated by mutagenesis to generate charge-separated states involving the B-branch cofactors. Overall, electron transfer to H_B is largely limited by the unfavorable energy of B_B and its limited coupling to P*. Electron transfer to Q_B can be observed but only when the normal electron transfer pathway along the A branch is blocked. The yield of electron transfer to Q_B is influenced by several factors, but most likely is limited by the rate being slow due to a high reorganization energy associated with formation of Q_B^-.

B. New Electron Transfer Reactions

Whereas most of the emphasis concerning electron transfer in reaction centers has been on elucidating the factors that control the rates and the asymmetry of electron transfer, other manipulations have introduced new pathways into the reaction center (see also Chapter 16, Jones). The focus in these experiments has been on exploiting the environment near P so as to introduce novel secondary donors. In *Rba. sphaeroides*, P is normally reduced by a water-soluble cytochrome c_2 (see Chapter 17, Axelrod et al.). In the absence of the cytochrome, P remains oxidized for

approximately 1 s until charge recombination from Q_B^- occurs. By comparison, after light excitation and charge separation, the oxidized primary electron donor of Photosystem II is rapidly reduced by a redox active tyrosine (Tyr 161 of the D1 subunit), which is usually identified as Y_Z. The electron transfer continues with Y_Z^+ being reduced by the Mn cluster where the four equivalents are stored until oxygen is evolved. Because of the relatively low midpoint potential of 500 mV for P, the bacterial reaction centers are normally not capable of oxidizing tyrosine or manganese. However, after hydrogen bonds are added to the dimer, P becomes highly oxidizing and is capable of oxidizing tyrosine residues, including a tyrosine introduced at a location analogous to that of Y_Z (Kálmán et al., 1999, 2003a,b; Narváez et al., 2002, 2004). Likewise, the modified reaction centers are capable of oxidizing manganese, which can be bound after amino acid residues acting as ligands are introduced (Fig. 8) (Thielges et al., 2005; Kálmán et al., 2005). These results demonstrate that new electron transfer pathways can be introduced, and such approaches can be used to delineate the complex evolutionary process by which anoxygenic photosynthetic complexes evolved into oxygenic complexes.

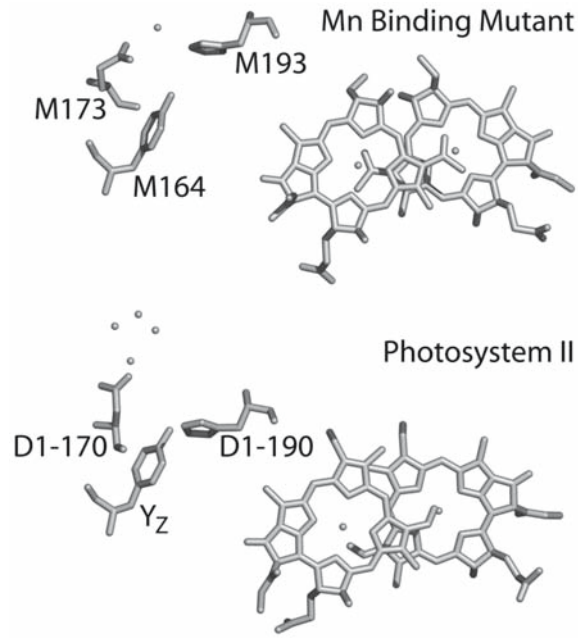

Fig. 8. Comparison of the three-dimensional structures of the Mn binding mutant (Thielges et al., 2005) and Photosystem II shows many similar features. In both cases, three critical amino acid residues are present, a carboxylate (M173 and D1-170), a tyrosine (M164 and Y_Z), and a histidine (M193 and D1-190). In addition, both complexes have a bound redox active Mn (a mononuclear and a Mn_4 cluster for the mutant and Photosystem II respectively; Mn atoms shown as small spheres) that can serve as a rapid secondary electron donor to the oxidized primary donor.

V. Conclusions

When a reaction center is excited by light, the interplay between the cofactors and the surrounding protein determines the route of electron transfer. The remarkable robustness of the reaction center to both biochemical manipulation and mutagenesis provides the opportunity to probe the features that influence electron transfer. The standard route down the A branch is observed to have the characteristics of energetics, coupling and dynamics that make it a durable electron transfer pathway. However multiple perturbation of the system makes possible other opportunistic reactions.

Acknowledgments

Our work is supported by the National Science Foundation, grant MCB0640002. We thank Aileen Taguchi for Fig. 6.

References

Alden RG, Parson WW, Chu ZT and Warshel A (1996) Orientation of the OH dipole of tyrosine (M)210 and its effect on electrostatic energies in photosynthetic bacterial reaction centers. J Phys Chem 100: 16761–16770

Allen JP and Williams JC (1995) Relationship between the oxidation potential of the bacteriochlorophyll dimer and electron transfer in photosynthetic reaction centers. J Bioenerg Biomembr 27: 275–283

Allen JP and Williams JC (2006) The influence of protein interactions on the properties of the bacteriochlorophyll dimer in reaction centers. In: Grimm B, Porra RJ, Rüdiger W and Scheer H (eds) Chlorophylls and Bacteriochlorophylls: Biochemistry, Biophysics, Functions and Applications (Advances in Photosynthesis and Respiration, Vol 25), pp 283–295. Springer, Dordrecht

Allen JP, Artz K, Lin X, Williams JC, Ivancich A, Albouy D, Mattioli TA, Fetsch A, Kuhn M and Lubitz W (1996) Effects of hydrogen bonding to a bacteriochlorophyll-bacteriopheophytin dimer in reaction centers from *Rhodobacter sphaeroides*. Biochemistry 35: 6612–6619

Allen JP, Williams JC, Graige MS, Paddock ML, Labahn A, Feher G and Okamura MY (1998) Free energy dependence of the direct charge recombination from the primary and secondary

quinones in reaction centers from *Rhodobacter sphaeroides*. Photosynth Res 55: 227–233

Arlt T, Dohse B, Schmidt S, Wachtveitl J, Laussermair E, Zinth W and Oesterhelt D (1996) Electron transfer dynamics of *Rhodopseudomonas viridis* reaction centers with a modified binding site for the accessory bacteriochlorophyll. Biochemistry 35: 9235–9244

Artz K, Williams JC, Allen JP, Lendzian F, Rautter J and Lubitz W (1997) Relationship between the oxidation potential and electron spin density of the primary electron donor in reaction centers from *Rhodobacter sphaeroides*. Proc Natl Acad Sci USA 94: 13582–13587

Breton J, Wakeham MC, Fyfe PK, Jones MR and Nabedryk E (2004) Characterization of the bonding interactions of Q_B upon photoreduction via A-branch or B-branch electron transfer in mutant reaction centers from *Rhodobacter sphaeroides*. Biochim Biophys Acta 1656: 127–138

Bylina EJ and Youvan DC (1988) Directed mutations affecting spectroscopic and electron transfer properties of the primary donor in the photosynthetic reaction center. Proc Natl Acad Sci USA 85: 7226–7230

Bylina EJ, Kirmaier C, McDowell L, Holten D and Youvan DC (1988) Influence of an amino-acid residue on the optical properties and electron transfer dynamics of a photosynthetic reaction centre complex. Nature 336: 182–184

Bylina EJ, Kolaczkowski SV, Norris JR and Youvan DC (1990) EPR characterization of genetically modified reaction centers of *Rhodobacter capsulatus*. Biochemistry 29: 6203–6210

Chen L, Holten D, Bocian DF and Kirmaier C (2004) Effects of hydrogen bonding and structure of the accessory bacteriochlorophylls on charge separation in *Rb. capsulatus* reaction centers. J Phys Chem B 108: 10457–10464

Chuang JI, Boxer SG, Holten D and Kirmaier C (2006) High yield of M-side electron transfer in mutants of *Rhodobacter capsulatus* reaction centers lacking the L-side bacteriopheophytin. Biochemistry 45: 3845–3851

Dahlbom MG and Reimers JR (2005) Successes and failures of time-dependent density functional theory for the low-lying excited states of chlorophylls. Mol Phys 103: 1057–1065

de Boer AL, Neerken S, de Wijn R, Permentier HP, Gast P, Vijgenboom E and Hoff AJ (2002) B-branch electron transfer in reaction centers of *Rhodobacter sphaeroides* assessed with site-directed mutagenesis. Photosynth Res 71: 221–239

Finkele U, Lauterwasser C, Zinth W, Gray KA and Oesterhelt D (1990) Role of tyrosine M210 in the initial charge separation of reaction centers of *Rhodobacter sphaeroides*. Biochemistry 29: 8517–8521

Frolov D, Wakeham MC, Andrizhiyevskaya EG, Jones MR and van Grondelle R (2005) Investigation of B-branch electron transfer by femtosecond time resolved spectroscopy in a *Rhodobacter sphaeroides* reaction centre that lacks the Q_A ubiquinone. Biochim Biophys Acta 1707: 189–198

Gehlen JN, Marchi M and Chandler D (1994) Dynamics affecting the primary charge transfer in photosynthesis. Science 263: 499–502

Goldsmith JO, King B and Boxer SG (1996) Mg coordination by amino acid side chains is not required for assembly and function of the special pair in bacterial photosynthetic reaction centers. Biochemistry 35: 2421–2428

Gray HB and Winkler JR (2005) Long-range electron transfer. Proc Natl Acad Sci USA 102: 3534–3539

Gunner MR, Nicholls A and Honig B (1996) Electrostatic potentials in *Rhodopseudomonas viridis* reaction centers: Implications for the driving force and directionality of electron transfer. J Phys Chem 100: 4277–4291

Haffa ALM, Lin S, Katilius E, Williams JC, Taguchi AKW, Allen JP and Woodbury NW (2002) The dependence of the initial electron-transfer rate on driving force in *Rhodobacter sphaeroides* reaction centers. J Phys Chem 106: 7376–7384

Haffa ALM, Lin S, Williams JC, Taguchi AKW, Allen JP and Woodbury NW (2003) High yield of long-lived B-side charge separation at room temperature in mutant bacterial reaction centers. J Phys Chem B 107: 12503–12510

Haffa ALM, Lin S, Williams JC, Bowen BP, Taguchi AKW, Allen JP and Woodbury NW (2004) Controlling the pathway of photosynthetic charge separation in bacterial reaction centers. J Phys Chem B 108: 4–7

Heller BA, Holten D and Kirmaier C (1995) Control of electron transfer between the L- and M-sides of photosynthetic reaction centers. Science 269: 940–945

Ishikita H, Loll B, Biesiadka J, Galstyan A, Saenger W and Knapp EW (2005) Tuning electron transfer by ester-group of chlorophylls in bacterial photosynthetic reaction center. FEBS Lett 579: 712–716

Ishikita H, Saenger W, Loll B, Biesiadka J and Knapp EW (2006) Energetics of a possible proton exit pathway for water oxidation in Photosystem II. Biochemistry 45: 2063–2071

Jackson JA, Lin S, Taguchi AKW, Williams JC, Allen JP and Woodbury NW (1997) Energy transfer in *Rhodobacter sphaeroides* reaction centers with the initial electron donor oxidized or missing. J Phys Chem B 101: 5747–5754

Jia Y, DiMagno TJ, Chan CK, Wang Z, Du M, Hanson DK, Schiffer M, Norris JR, Fleming GR and Popov MS (1993) Primary charge separation in mutant reaction centers of *Rhodobacter capsulatus*. J Phys Chem 97: 13180–13191

Johnson ET and Parson WW (2002) Electrostatic interactions in an integral membrane protein. Biochemistry 41: 6483–6494

Johnson ET, Müh F, Nabedryk E, Williams JC, Allen JP, Lubitz W, Breton J and Parson WW (2002) Electronic and vibronic coupling of the special pair of bacteriochlorophylls in photosynthetic reaction centers from wild-type and mutant strains of *Rhodobacter sphaeroides.* J Phys Chem B 106: 11859–11869

Kálmán L, LoBrutto R, Allen JP and Williams JC (1999) Modified reaction centres oxidize tyrosine in reactions that mirror Photosystem II. Nature 402: 696–699

Kálmán L, Williams JC and Allen JP (2003a) Proton release upon oxidation of tyrosine in reaction centers from *Rhodobacter sphaeroides*. FEBS Lett 545: 193–198

Kálmán L, LoBrutto R, Narváez AJ, Williams JC and Allen JP (2003b) Correlation of proton release and electrochromic shifts of the optical spectrum due to oxidation of tyrosine in reaction centers from *Rhodobacter sphaeroides*. Biochemistry 42: 13280–13286

Kálmán L, Thielges MC, Williams JC and Allen JP (2005) Proton release due to manganese binding and oxidation in modified bacterial reaction centers. Biochemistry 44: 13266–13273

Kanchanawong P, Dahlbom MG, Treynor TP, Reimers JR, Hush NS and Boxer SG (2006) Charge delocalization in the special-pair radical cation of mutant reaction centers of *Rhodobacter sphaeroides* from Stark spectra and nonadiabatic spectral simulations. J Phys Chem B 110: 18688–18702

Katilius E, Turanchik T, Lin S, Taguchi AKW and Woodbury NW

(1999) B-side electron transfer in a *Rhodobacter sphaeroides* reaction center mutant in which the B-side monomer bacteriochlorophyll is replaced with bacteriopheophytin. J Phys Chem B 103: 7386–7389

Katilius E, Katiliene Z, Lin S, Taguchi AKW and Woodbury NW (2002a) B side electron transfer in a *Rhodobacter sphaeroides* reaction center mutant in which the B side monomer bacteriochlorophyll is replaced with bacteriopheophytin: Low-temperature study and energetics of charge-separated states. J Phys Chem B 106: 1471–1475

Katilius E, Katiliene Z, Lin S, Taguchi AKW and Woodbury NW (2002b) B-side electron transfer in the HE(M182) reaction center mutant from *Rhodobacter sphaeroides*. J Phys Chem B 106: 12344–12350

Katilius E, Babendure JL, Katiliene Z, Lin S, Taguchi AKW and Woodbury NW (2003) Manipulations of the B-side charge-separated states' energetics in the *Rhodobacter sphaeroides* reaction center. J Phys Chem B 107: 12029–12034

Katilius E, Babendure JL, Lin S and Woodbury NW (2004) Electron transfer dynamics in *Rhodobacter sphaeroides* reaction center mutants with a modified ligand for the monomer bacteriochlorophyll on the active side. Photosynth Res 81: 165–180

Kee HL, Laible PD, Bautista JA, Hanson DK, Holten D and Kirmaier C (2006) Determination of the rate and yield of B-side quinone reduction in *Rhodobacter capsulatus* reaction centers. Biochemistry 45: 7314–7322

Khatypov RA, Vasilieva LG, Fufina TY, Bolgarina TI and Shuvalov VA (2005) Substitution of isoleucine L177 by histidine affects the pigment composition and properties of the reaction center of the purple bacterium *Rhodobacter sphaeroides*. Biochemistry (Moscow) 70: 1527–1533

King BA, de Winter A, McAnaney TB and Boxer SG (2001) Excited state energy transfer pathways in photosynthetic reaction centers. 4. Asymmetric energy transfer in the heterodimer mutant. J Phys Chem B 105: 1856–1862

Kirmaier C, Holten, D, Bylina EJ and Youvan DC (1988) Electron transfer in a genetically modified bacterial reaction center containing a heterodimer. Proc Natl Acad Sci USA 85: 7562–7566

Kirmaier C, Gaul D, DeBey R, Holten D and Schenck CC (1991) Charge separation in a reaction center incorporating bacteriochlorophyll for photoactive bacteriopheophytin. Science 251: 922–927

Kirmaier C, Weems D and Holten D (1999) M-side electron transfer in reaction center mutants with a lysine near the nonphotoactive bacteriochlorophyll. Biochemistry 38: 11516–11530

Kirmaier C, He C and Holten D (2001) Manipulating the direction of electron transfer in the bacterial reaction center by swapping Phe for Tyr near $BChl_M$ (L181) and Tyr for Phe near $BChl_L$ (M208). Biochemistry 40: 12132–12139

Kirmaier C, Cua A, He C, Holten D and Bocian DF (2002a) Probing the M-branch electron transfer and cofactor environment in the bacterial photosynthetic reaction center by addition of a hydrogen bond to the M-side bacteriopheophytin. J Phys Chem B 106: 495–503

Kirmaier C, Laible PD, Czarnecki K, Hata AN, Hanson DK, Bocian DF and Holten D (2002b) Comparison of M-side electron transfer in *Rb. sphaeroides* and *Rb. capsulatus* reaction centers. J Phys Chem B 106: 1799–1808

Kirmaier C, Laible PD, Hanson DK and Holten D (2003) B-side charge separation in bacterial photosynthetic reaction centers: nanosecond time scale electron transfer from H_B^- to Q_B. Biochemistry 42: 2016–2024

Kirmaier C, Laible PD, Hanson DK and Holten D (2004) B-side electron transfer to form $P^+H_B^-$ in reaction centers from the F(L181)Y/Y(M208)F mutant of *Rhodobacter capsulatus*. J Phys Chem B 108: 11827–11832

Kirmaier C, Bautista JA, Laible PD, Hanson DK and Holten D (2005) Probing the contribution of electronic coupling to the directionality of electron transfer in photosynthetic reaction centers. J Phys Chem B 109: 24160–24172

Laible PD, Kirmaier C, Udawatte CSM, Hofman SJ, Holten D and Hanson DK (2003) Quinone reduction via secondary B-branch electron transfer in mutant bacterial reaction centers. Biochemistry 42: 1718–1730

Li Y, Lucas MG, Konovalova T, Abbott B, MacMillan F, Petrenko A, Sivakumar V, Wang R, Hastings G, Gu F, van Tol J, Brunel LC, Timkovich R, Rappaport F and Redding K (2004) Mutation of the putative hydrogen-bond donor to P_{700} of Photosystem I. Biochemistry 43: 12634–12647

Li Y, van der Est A, Lucas MG, Ramesh VM, Gu F, Petrenko A, Lin S, Webber AN, Rappaport F and Redding K (2006) Directing electron transfer within Photosystem I by breaking H-bonds in the cofactor branches. Proc Natl Acad Sci USA 103: 2144–2149

Lin J and Beratan DN (2005) Simulation of electron transfer between cytochrome c_2 and the bacterial photosynthetic reaction center: Brownian dynamics analysis of the native proteins and double mutants. J Phys Chem B 109: 7529–7534

Lin J, Balabin IA and Beratan DN (2005) The nature of aqueous tunneling pathways between electron-transfer proteins. Science 310: 1311–1313

Lin S, Katilius E, Haffa ALM, Taguchi AKW and Woodbury NW (2001) Blue light drives B-side electron transfer in bacterial photosynthetic reaction centers. Biochemistry 40: 13767–13773

Lin S, Katilius E, Taguchi AKW and Woodbury NW (2003) Excitation energy transfer from carotenoid to bacteriochlorophyll in the photosynthetic purple bacterial reaction center of *Rhodobacter sphaeroides*. J Phys Chem B 107: 14103–14108

Lin X, Murchison HA, Nagarajan V, Parson WW, Allen JP and Williams JC (1994a) Specific alteration of the oxidation potential of the electron donor in reaction centers from *Rhodobacter sphaeroides*. Proc Natl Acad Sci USA 91: 10265–10269

Lin X, Williams JC, Allen JP and Mathis P (1994b) Relationship between rate and free energy difference for electron transfer from cytochrome c_2 to the reaction center in *Rhodobacter sphaeroides.* Biochemistry 33: 13517–13523

Marcus RA and Sutin N (1985) Electron transfers in chemistry and biology. Biochim Biophys Acta 811: 265–322

McDowell LM, Gaul D, Kirmaier C, Holten D and Schenck CC (1991) Investigation into the source of electron transfer asymmetry in bacterial reaction centers. Biochemistry 30: 8315–8322

Middendorf TR, Mazzola LT, Lao K, Steffen MA and Boxer SG (1993) Stark effect (electroabsorption) spectroscopy of photosynthetic reaction centers at 1.5 K: Evidence that the special pair has a large excited-state polarizability. Biochim Biophys Acta 1143: 223–234

Miyashita O, Okamura MY and Onuchic JN (2005) Interprotein electron transfer from cytochrome c_2 to photosynthetic reaction

center: Tunneling across an aqueous interface. Proc Natl Acad Sci USA 102: 3558–3563

Moore LJ and Boxer SG (1998) Inter-chromophore interactions in pigment-modified and dimer-less bacterial photosynthetic reaction centers. Photosynth Res 55: 173–180

Müh F, Williams, JC, Allen JP and Lubitz W (1998) A conformational change of the photoactive bacteriopheophytin in reaction centers from *Rhodobacter sphaeroides*. Biochemistry 37: 13066–13074

Müh F, Lendzian F, Roy M, Williams JC, Allen JP and Lubitz W (2002) Pigment-protein interactions in bacterial reaction centers and their influence on oxidation potential and spin density distribution of the primary donor. J Phys Chem B 106: 3226–3236

Murchison HA, Alden RG, Allen JP, Peloquin JM, Taguchi AKW, Woodbury NW and Williams JC (1993) Mutations designed to modify the environment of the primary electron donor of the reaction center from *Rhodobacter sphaeroides*: Phenylalanine to leucine at L167 and histidine to phenylalanine at L168. Biochemistry 32: 3498–3505

Nagarajan V, Parson WW, Gaul D and Schenck C (1990) Effect of specific mutations of tyrosine-(M)210 on the primary photosynthetic electron-transfer process in *Rhodobacter sphaeroides*. Proc Natl Acad Sci USA 87: 7888–7892

Narváez AJ, Kálmán L, LoBrutto R, Allen JP and Williams JC (2002) Influence of the protein environment on the properties of a tyrosyl radical in reaction centers from *Rhodobacter sphaeroides*. Biochemistry 41: 15253–15258

Narváez AJ, LoBrutto R, Allen JP and Williams JC (2004) Trapped tyrosyl radical populations in modified reaction centers from *Rhodobacter sphaeroides*. Biochemistry 43: 14379–14384

Noy D, Moser CC and Dutton PL (2006) Design and engineering of photosynthetic light-harvesting and electron transfer using length, time, and energy scales. Biochim Biophys Acta 1757: 90–105

Paddock ML, Chang C, Xu Q, Abresch EC, Axelrod HL, Feher G and Okamura MY (2005) Quinone (Q_B) reduction by B-branch electron transfer in mutant bacterial reaction centers from *Rhodobacter sphaeroides*: quantum efficiency and X-ray structure. Biochemistry 44: 6920–6928

Paddock ML, Flores M, Isaacson R, Chang C, Abresch EC, Selvaduray P and Okamura MY (2006) Trapped conformational states of semiquinone ($D^{+\cdot}Q_B^{\cdot}$) formed by B-branch electron transfer at low temperature in *Rhodobacter sphaeroides* reaction centers. Biochemistry 45: 14032–14042

Parson WW, Chu ZT and Warshel A (1990) Electrostatic control of charge separation in bacterial photosynthesis. Biochim Biophys Acta 1017: 251–272

Plato M, Lendzian F, Lubitz W and Möbius K (1992) Molecular orbital study of electronic asymmetry in primary donors of bacterial reaction centers. In: Breton J and Verméglio A (eds) The Photosynthetic Bacterial Reaction Center II: Structure, Spectroscopy, and Dynamics, pp 109–118. Plenum, New York

Potter JA, Fyfe PK, Frolov D, Wakeham MC, van Grondelle R, Robert B and Jones MR (2005) Strong effects of an individual water molecule on the rate of light-driven charge separation in the *Rhodobacter sphaeroides* reaction center. J Biol Chem 280: 27155–27164

Reimers JR and Hush NS (2004) A unified description of the electrochemical, charge distribution, and spectroscopic properties of the special-pair radical cation in bacterial photosynthesis. J Am Chem Soc 126: 4132–4144

Robles SJ, Breton J and Youvan DC (1990) Partial symmetrization of the photosynthetic reaction center. Science 248: 1402–1405

Spiedel D, Jones MR and Robert B (2002) Tuning of the redox potential of the primary electron donor in reaction centres of purple bacteria: Effects of amino acid polarity and position. FEBS Lett 527: 171–175

Stocker JW, Taguchi AKW, Murchison HA, Woodbury NW and Boxer SG (1992) Spectroscopic and redox properties of sym1 and (M)F195H: *Rhodobacter capsulatus* reaction center symmetry mutants which affect the initial electron donor. Biochemistry 31: 10356–10362

Sumi H and Marcus RA (1986) Dielectric relaxation and intramolecular electron transfers. J Chem Phys 84: 4272–4276

Thielges M, Uyeda G, Cámara-Artigas A, Kálmán L, Williams JC and Allen JP (2005) Design of a redox-linked active metal site: Manganese bound to bacterial reaction centers at a site resembling that of Photosystem II. Biochemistry 44: 7389–7394

Treynor TP, Yoshina-Ishii C and Boxer SG (2004) Probing excited-state electron transfer by resonance Stark spectroscopy: 4. Mutations near B_L in photosynthetic reaction centers perturb multiple factors that affect $B_L^* \rightarrow B_L^+H_L^-$. J Phys Chem B 108: 13523–13535

van Brederode ME, van Stokkum IHM, Katilius E, van Mourik F, Jones MR and van Grondelle R (1999) Primary charge separation routes in the BChl:Bphe heterodimer reaction centers of *Rhodobacter sphaeroides*. Biochemistry 38: 7545–7555

Wakeham MC and Jones MR (2005) Rewiring photosynthesis: Engineering wrong-way electron transfer in the purple bacterial reaction centre. Biochem Soc Trans 33: 851–857

Wakeham MC, Goodwin MG, McKibbin C and Jones MR (2003) Photo-accumulation of the $P^+Q_B^-$ radical pair state in purple bacterial reaction centres that lack the Q_A ubiquinone. FEBS Lett 540: 234–240

Wakeham MC, Breton J, Nabedryk E and Jones MR (2004) Formation of a semiquinone at the Q_B site by A- or B-branch electron transfer in the reaction center from *Rhodobacter sphaeroides*. Biochemistry 43: 4755–4763

Wang H, Lin S and Woodbury NW (2006) Electronic transitions of the Soret band of reaction centers from *Rhodobacter sphaeroides* studied by femtosecond transient absorbance spectroscopy. J Phys Chem B 110: 6956–6961

Wang H, Lin S, Allen JP, Williams JC, Blankert S, Laser C and Woodbury NW (2007) Protein dynamics control the kinetics of initial electron transfer in photosynthesis. Science 316: 747–750

Warshel A, Chu ZT and Parson WW (1989) Dispersed polaron simulations of electron transfer in photosynthetic reaction centers. Science 246: 112–116

Watson AJ, Fyfe PK, Frolov D, Wakeham MC, Nabedryk E, van Grondelle R, Breton J and Jones MR (2005) Replacement or exclusion of the B-branch bacteriopheophytin in the purple bacterial reaction centre: The H_B cofactor is not required for assembly or core function of the *Rhodobacter sphaeroides* complex. Biochim Biophys Acta 1710: 34–46

Webber AN and Lubitz W (2001) P700: The primary electron donor of Photosystem I. Biochim Biophys Acta 1507: 61–79

Williams JC, Alden RG, Murchison HA, Peloquin JM, Woodbury NW and Allen JP (1992) Effects of mutations near the bacteriochlorophylls in reaction centers from *Rhodobacter*

sphaeroides. Biochemistry 31: 11029–11037

Williams JC, Haffa ALM, McCulley JL, Woodbury NW and Allen JP (2001) Electrostatic interactions between charged amino acid residues and the bacteriochlorophyll dimer in reaction centers from *Rhodobacter sphaeroides*. Biochemistry 40: 15403–15407

Williams JC, Paddock ML, Way YP and Allen JP (2007) Changes in metal specificity due to iron ligand substitutions in reaction centers from *Rhodobacter sphaeroides*. Appl Magn Reson 31: 45–58

Witt H, Schlodder E, Teutloff C, Niklas J, Bordignon E, Carbonera D, Kohler S, Labahn A and Lubitz W (2002) Hydrogen bonding to P700: site-directed mutagenesis of threonine A739 of Photosystem I in *Chlamydomonas reinhardtii*. Biochemistry 41: 8557–8569

Yakovlev AG, Jones MR, Potter JA, Fyfe PK, Vasilieva LG, Shkuropatov AY and Shuvalov VA (2005) Primary charge separation between P* and B_A: Electron-transfer pathways in native and mutant GM203L bacterial reaction centers. Chem Phys 319: 297–307

Yanagi K, Shimizu M, Hashimoto H, Gardiner AT, Roszak AW and Cogdell RJ (2005) Local electrostatic field induced by the carotenoid bound to the reaction center of the purple photosynthetic bacterium *Rhodobacter sphaeroides*. J Phys Chem B 109: 992–998